Chemical Science

Accepted Manuscript

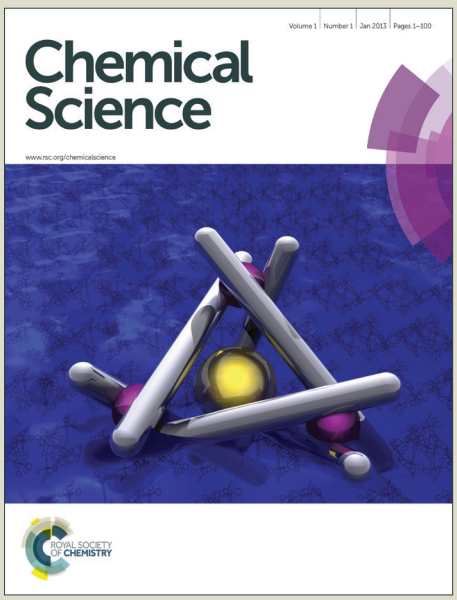

ROYAL SOCIETY OF CHEMISTRY

www.rsc.org/chemicalscience

Chemical Science

ARTICLE

Dielectric-Dependent Electron Transfer Behaviour of Cobalt Hexacyanides in Solid Solution of Sodium Chloride

Received 00th January 20xx,
Accepted 00th January 20xx

DOI: 10.1039/x0xx00000x

www.rsc.org/

Di Huang, Yiliang Zhu, Ya-Qiong Su, Jie Zhang, Lianhuan Han, De-Yin Wu, Zhong-Qun Tian, Dongping Zhan*

Here we emphasis the importance of dielectric environment on the electron transfer bahavior in the interfacial electrochemical systems. Through doping cobalt hexacyanide ($Co(CN)_6^{3-}$) into single microcrystals of sodium chloride (NaCl), for the first time, we obtained the direct electrochemistry of $Co(CN)_6^{3-}$ which is hardly obtained in either aqueous or the conventional nonaqueous solutions. DFT calculations elucidate that, as $Co(CN)_6^{3-}$ anions occupy the lattice units of $NaCl_6^{5-}$ in NaCl microcrystal, the redox energy barrier of $Co(CN)_6^{3-/4-}$ is decreased dramatically due to the low dielectric constant of NaCl. Meanwhile, the low-spin $Co(CN)_6^{4-}$ anions are stabilized in the lattices of NaCl microcrystal. The results also show that NaCl microcrystal is a potential solvent for solid-state electrochemistry at ambient temperature.

Introduction

The dielectric property of solvent, crucial in the interfacial electron transfer reactions, has been paid little attention in the initiative design of electrochemical systems. In principle, the hexacyanides of transition metals have good capability of electron transfer due to both the multivalent central cations and the homogeneous charge distribution. For example, potassium ferricyanide ($K_3Fe(CN)_6$), with a standard electrode potential of $Fe(CN)_6^{3-/4-}$ couple is 0.361 V versus the normal hydrogen electrode (NHE) at 25 °C, is used widely as a classic redox couple in electrochemistry.[1] The reversible electron transfer behavior underlies determination of the effective area of glassy carbon electrodes.[2] However, despite the similar molecular structure of cobalt hexacyanide ($Co(CN)_6^{3-}$) to $Fe(CN)_6^{3-}$, redox behavior of $Co(CN)_6^{3-}$ in conventional aqueous or nonaqueous solutions have been seldom reported to date. Although theoretical calculation implies the possiblity if dielectric constant of electrolyte solution is decreased to 5, this indication has never been validated experimentally due to the lack of qualified solvent.[3] Since the dielectric constant of NaCl (ε: 6.0 F/m) is very close to 5 F/m, based on our previous research on solid solution of NaCl microcrystals,[4] we synthesize $Co(CN)_6^{3-}$ doped NaCl microcrytals and observed the direct electrochemical behavior of $Co(CN)_6^{3-/4-}$ in the dielectric environment of NaCl microcrystal.

We have developed scanning electrochemical cell microscopy (SECCM) to culture NaCl solid-solution microcrystals wherein redox couples are doped as solute.[4] Derived from scanning electrochemical microscopy, SECCM employs a micropipette with a micro- or nano-meter sized orifice as both scanning tip and electrochemical cell (Figure 1)[5], which has been proved as an effective technique in the research areas including the reaction kinetics,[6] micro- or nano-patterning and imaging,[5e,7] local corrosion or deposition,[8] and also the catalyst screening.[9] It was found that the $Fe(CN)_6^{3-/4-}$/NaCl solid-solution microcrystals have excellent solid-state redox behaviors in the absence of any liquid electrolyte, because the doped redox couple makes them electronic conductor while the crystal defects make them ionic conductor.[4a,4b] Here, for the first time, we report the dielectric environment dependent, direct electron transfer behavior of $Co(CN)_6^{3-/4-}$ in NaCl microcrystals.

Experimental Section

Chemicals, Materials, and Instruments

NaCl and $Na_3Co(CN)_6$ were analytical grade or better (Sinopharm Co., China). All aqueous solutions were prepared with deionized water (18.2 MΩ, Milli-Q, Millipore Corp.). The borosilicate micropipets (o.d., 1.2 mm; i.d., 0.8 mm) with orifice of 3~10 μm diameter were prepared with a programmed laser puller PS-2000 (Sutter Co., USA) as reported previously.[4,15] The Au and Pt thin-film coated glass slides were prepared through magnetron sputter plating (JC500-3/D, Chengdu Vacuum Equipment Co., China). The ITO glass slides are a kind gift from Prof. Bin Ren at Xiamen University. Before experiments, the slides were cleaned with acetone and deionized water for several times and dried with pure nitrogen gas. A scanning electron microscope (SEM, Hitachi High-Technologies Co., Japan) was employed to obtain geometric topography and elementary analysis of the single microcrystals.

State Key Laboratory of Physical Chemistry of Solid Surfaces, and Department of Chemistry, College of Chemistry and Chemical Engineering, Xiamen University, 422 Siming South Road, Xiamen 361005, China.
Corresponding Author: Prof. Dr. Dongping Zhan
E-mail: dpzhan@xmu.edu.cn

Confocal Raman spectrum experiments were performed with a Renishaw inVia Raman microscope (Renishaw Co., British) to confirm the composition of microcrystalline solution. All electrochemical experiments were performed with the SECM workstation CHI920c (CHI Instrument Co., USA).

Culture and assembly of $Na_3Co(CN)_6$/NaCl microcrystals

We have developed SECCM technique to culture and to assembly $Na_3Co(CN)_6$/NaCl microcrystal.[4] A micropipette with a micrometer sized orifice acts as both the scanning tip and the electrolytic cell. An Ag/AgCl wire was inserted into the micropipette as both the counter and reference electrodes. A conductive substrate, such as ITO, Au, or Pt thin-film-coated glass slide, was the working electrode. With the help of the video camera, the micropipette was moved to contact with the conductive substrate. Since the tip and substrate contact with each other through a ~picoliter or ~femtoliter drop of electrolyte solution, electrochemical reactions were confined in the small volume of microdrop between the tip and the substrate. Actually, the spatial resolution of SECCM depends on the size of the microdrop. When the tip was scanning, the whole electrochemical microsystem moved. Due to the evaporation of water, the microcrystal can be obtained on the substrate. In order to form an electrochemical system, the microcrystal was assembled on the gap between a pair of gold microwire, which is deposited on a microchip made by lithography techniques.

Theoretical Calculations

The quantum-chemical calculations were carried out for geometry optimizations at the density functional theory (DFT) level with the hybrid functional B3LYP by performing the Gaussian 09 package.[16] For C and N atoms, the basis set used was 6-311+G**.[17] For Co atom, the small core pseudopotential basis set LanL2DZ was adopted.[18] To take the solvent effect into account, the Polarized Continuum Model (PCM) was used in all calculations.[19] The dielectric constant ε is 78.3 F/m for water as well as 6.0 F/m for NaCl solid-solution microcrystal. The Potential Energy Curves (PES) were fitted by optimizing and obtaining some special single point energies along the reaction coordinates.

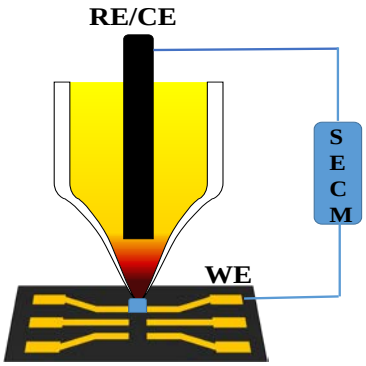

Figure 1 Schematic diagram of the assembly of $Co(CN)_6^{3-}$/NaCl microcrystals into an electrochemical chip by SECCM: a microcapillary with a micrometer-sized orifice was employed as the scanning tip and the electrochemical cell, the reference and counter electrodes were inserted in the microcapillary, and a pair of gold microelectrods on the electrochemical microchip as the working electrode.

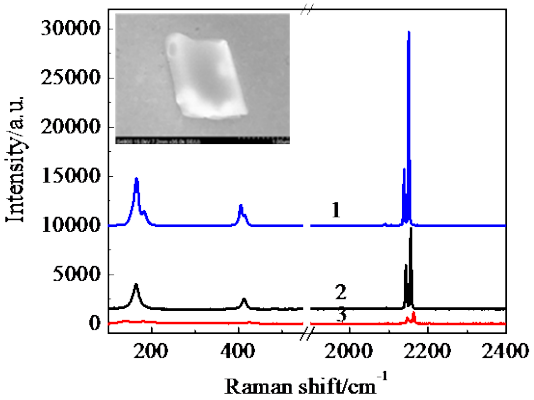

Figure 2 The confocal Raman spectra of the pure $Na_3Co(CN)_6$ crystals (curve 1), and the single $Na_3Co(CN)_6$/NaCl solid solution microcrystals with initial $Na_3Co(CN)_6$ concentration of 10 mM (curve 2) and 1 mM (Curve 3), the concentration of NaCl in the precusor soluition is 50 mM. The inset is SEM image of single $Na_3Co(CN)_6$/NaCl microcrystal.

Results and Discussion

As depicted in Figure 1, the micropipette contacts with the conductive substrate through an electrolyte microdrop with a volume of pico or femto liter to construct the electrochemical microsystem. Water will evaporate since the microdrop is exposed to the atmosphere. From the Kelvin equation:[10]

$$RT\ln(P/P_0) = 2\gamma M/\rho r \quad (1)$$

The smaller the r is, the higher the P is, and the faster the water evaporates. Where P is the actual evaporation pressure, P_0 the saturated evaporation pressure, γ the surface tension, M the molecular weight of the electrolyte, ρ the density of the electrolyte，r the radius of the microdrop, R the gas constant and T the absolute temperature. Cyclic voltammetry with a scanning rate of 50 mV/s and a scan range between 0 mV and 500 mV is performed to modulate the surface tension and, therefore, the process of water evaporation. In general, it takes a few cycles to form a well-shaped microcrystal (the insert in Figure 2). If the electrochemical modulation were not applied, it would take more time for the microcrystal growth. Meanwhile, the shape of the microcrystals would become uncontrollable as reported previously.[4]

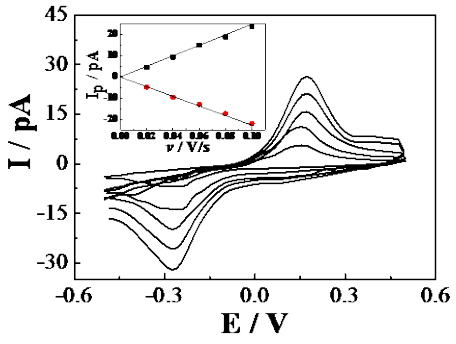

Figure 3 Cyclic voltammetric behavior of $Co(CN)_6^{3-/4-}$ in NaCl microcrystals in the dry box. The precursor solution for culturing NaCl microcrystals containing 10 mM $Co(CN)_6^{3-}$ and 50 mM NaCl. The insert shows the linear relationship between the peak current and the scanning rate.

Since the lattice size of $Na_3Co(CN)_6$ (9.39 Å) is very close to that of NaCl (9.2 Å), which means that the $Co(CN)_6^{3-}$ units can take the place of $NaCl_6^{5-}$ units and dope in the NaCl microcrystal to form a solid solution.[11, 12] As the valence of Co^{3+} is higher than Na^+, to achieve electroneutrality, two Na^+ vacancies are left in the neighboring $NaCl_6^{5-}$ units. That means the $Na_3Co(CN)_6$/NaCl solid solution is a Na^+ ionic conductor. Due to the difference between the lattice sizes of $Na_3Co(CN)_6$ and NaCl (2.06%), to some extent, the microcrystals have a characteristics of twin crystal. The crystal defects including both vacancies and interstitials are essential to improve the ionic conductivity of $Na_3Co(CN)_6$/NaCl solid-solution microcrystals.[13] The component of $Co(CN)_6^{3-}$ in the NaCl microcrystal is verified by the confocal Raman spectra (Figure 2). The charecteristic bands obtained from the microcrystals are in accordance with that of pure $Na_3Co(CN)_6$ crystals. The bands at 116 $cm^{-1}$and 405 cm^{-1} are assigned to the Fe-C stretching as well as the bands at 2139 $cm^{-1}$and 2151 cm^{-1} to the C≡N stretching. The band strengths is relative to the initial concentration of $Na_3Co(CN)_6$ in the precusor solution.

Single $Na_3Co(CN)_6$/NaCl microcrystal is assembled into the gap between a pair of gold microwire on a microchip by SECCM to construct an all-in-solid electrochemical system as reported previously (Figure 1a).[4] Well-defined voltammetric behaviors of $Co(CN)_6^{3-}$ in NaCl microcrystal was obtained as shown in Figure 3. The redox process can be formulated as:

$$Co(CN)_6^{3-} + e \rightleftharpoons Co(CN)_6^{4-} \quad (2)$$

The difference of peak potentials between the anodic and cathodic processes is rather big (~450 mV), which indicates the electron transfer reaction is irreversible and kinetically slow. In other words, both the anodic and the cathodic process need a large overpotential. From the insert of Figure 3, the peak current has a good linear relationship with the scanning rate. Because the redox units $Co(CN)_6^{3-}$ are trapped in the lattices of NaCl microcrystal, the electron transfer occurs through electron hopping or self-exchange between neighbouring $Co(CN)_6^{3-}$ unites. Meanwhile, to maintain the electroneutrality of NaCl microcrystal, the local charges caused by electron transfer are compensated by the diffusion and electromigration of counterion Na^+. Suppose the electron transfer behavior is similar to the thin-layer voltametry as analyzed before, the rlationship between peak current and the scanning rate for an irreversible process can be expressed as:[4a,4b,14]

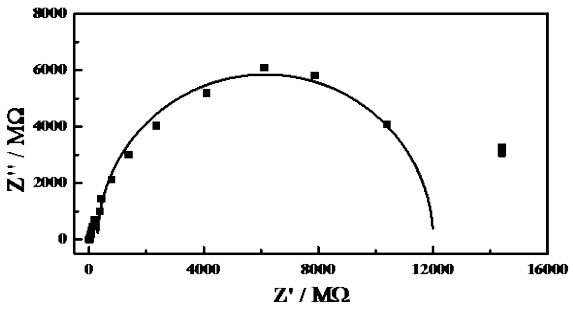

Figure 4 The electrochemical impedance spectroscopy of redox couple $Co(CN)_6^{3-/4-}$ in NaCl microcrystals. The initial concentration of $Co(CN)_6^{3-}$ for crystal culture is 10 mM.

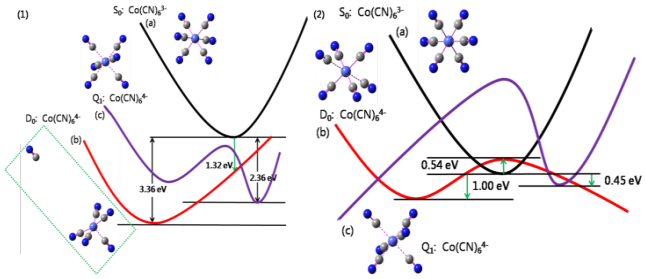

Figure 5 (1) Qualitative potential energy curves of (a) $Co(CN)_6^{3-}$ anion (S_0, black line), (b) $Co(CN)_6^{4-}$ anion in the low-spin state (D_0, red line), and (c) $Co(CN)_6^{4-}$ anion in the high-spin state (Q_1, purple line) at the PCM-B3LYP/6-311+G**/LANL2DZ level in aqueous solution (ε: 78.3 F/m). (2) Potential energy curves of (a) $Co(CN)_6^{3-}$ anion (S_0, black line), (b) $Co(CN)_6^{4-}$ anion in the low-spin state (D_0, red line), and (c) $Co(CN)_6^{4-}$ anion in the high-spin state (Q_1, purple line) at the PCM-B3LYP/6-311+G**/LANL2DZ level in NaCl solid solution (ε: 6.0 F/m).

$$i_p = \frac{\alpha n^2 F^2 V v C^*}{2.718RT} \quad (3)$$

Where i_p is the peak current, α the charge transfer coeeficient, n the stoichiometric charge transfer number, F the Faraday constant, V the volume of the microcrystal, v the scanning rate, C* the bulk concentration of reactant, R and T same as inducated in Equation (1). The dimension of the single $Na_3Co(CN)_6$/NaCl microcrystals are about 2μm × 2μm × 2μm. If α is 0.5, the apparent concentration of $Co(CN)_6^{3-}$ in NaCl microcrystals can be estimated as 4.3×10^{-5} mol/cm^3.

Furthermore, the experiment of electrochemical impedance spectroscopy (EIS) was performed to obtain the kinetic rate of electron transfer (shown in Figure 4). Considering the redox process of $Co(CN)_6^{3-}$ is a simple one-electron reansfer reaction as shown in Equation (2), in the range of high frenquency, the following equation should be applied:[1]

$$(Z' - R_u - R_{et}/2)^2 + Z''^2 = (R_{et}/2)^2 \quad (4)$$

Where R_u is the Ohm resistance of the single microcrystal, R_{et} is the electron transfer resistance, Z'and Z'' are the real and imaginary part of the impedance, respectively. The electron transfer resistance (R_{et}) is derived as 1.21×10^{10}Ω. By using the geometric parameters and the apparent concentration of $Co(CN)_6^{3-}$ obtained by cyclic voltammetry, the kinetic rate of electron transfer, k_{et}, is calculated as 1.24×10^{-5} cm/s. However, Figure 4 can't provide the mass transfer information, i.e., the diffusion of the counterion Na^+ in the NaCl microrystal. Our previous study shows the apparent diffusion coefficient (D) of Na^+ in $Na_3Fe(CN)_6$/NaCl microcrystals is 8.05×10^{-8} cm^2/s.[4b] Considering the similarity of $Na_3Co(CN)_6$/NaCl microcrystals, the mass transfer rate, k_{mt}, is estimated as 4.0×10^{-4} cm/s if the thickness of diffusion layer (δ) is 2 μm (k_{mt} = D/δ). Note that the mass transfer rate is much higher than the electron transfer rate ($k_{mt} > 20k_{et}$), it can be concluded that the rate-determining step (rds) of the redox reaction of $Co(CN)_6^{3-}$ in NaCl microcrystal is the electron propagations in the NaCl microcrystals. The EIS results elucidates, in turn, the validity of the "irreversible" hypothesis in the discussion section of cyclic voltammetry.

It should be noted that this reaction can't be observed in conventional solvents even if mercury electrode was employed to extend the potential window more negative.[3] To elucidate

the unique redox behavior of $Co(CN)_6^{3-/4-}$ in NaCl microcrystal, theoretical calculations were performed by density functional theory (DFT) method. Figure 5 gives the potential energy curves (PEC) of electrochemical reduction process of $Co(CN)_6^{3-}$ anion in both aqueous solution (ε: 78.3 F/m) and NaCl solid solution (ε: 6.0 F/m). In aqueous solution, the predicted reorganization energy λ is 2.04 eV after accepting an electron to form the low-spin $Co(CN)_6^{4-}$ anion, which is instable and quickly decomposed into $Co(CN)_5^{3-}$ and CN- ions by the rupture of Co-CN bond due to the introduction of an electron. Figure 5.1b gives the corresponding optimization structure, and the distance between the dissociated CN- and $Co(CN)_5^{3-}$ anion is 10.57 Å. It is obvious that there is no bonding interaction between them. However, the high-spin $Co(CN)_6^{4-}$ anion is relative stable and keep the original geometric symmetry with the reorganization energy of 1.59 eV. It should be noted that the S_0 and D_0 PECs have no cross points along the electron transfer reaction coordinate and, if injected an electron, the relaxation process of $Co(CN)_6^{3-}$ anion would be irreversible with an enormous stabilization energy of 3.36 eV. In summary, in aqueous solution, the electrochemical reduction product of $Co(CN)_6^{3-}$ anion prefers to be the low-spin $Co(CN)_5^{3-}$ and CN- ion and the predicted reduction potential is about -0.98 V vs. NHE. Unfortunately, in aqueous solution this redox behavior hasn't been observed experimentally.[3]

However, in NaCl solid-solution microcrystal, the S_0, D_0 and Q_1 PEC are intersectional. For the reduction of $Co(CN)_6^{3-}$ anion, the reorganization energy is about 1.54 eV. The injected electron just climbs over a low energy barrier (< 0.54 eV) to enter the D_0 PEC and relaxes into the product, the low-spin $Co(CN)_6^{4-}$ anion, which is stabilized and keeps the original coordination number in the dielectric environment of NaCl microcrystal. Meanwhile, the oxidation energy barrier of reverse process is just between 1.00 and 1.54 eV. The low dielectric constant (ε: 6.0 F/m) leads to a smaller stabilization energy of 1.00 eV and, consequently, an electrochemical redox process of $Co(CN)_6^{3-/4-}$ couple. It can be concluded that the dielectric environment plays a vital role in not only the thermodynamic possibility but also the electrode kinetics of electron transfer processes. The NaCl solid-solution microcrystal can provide suitable dielectric environment for the hexacyanides of transition metals which are expected to have good electron transfer properties but, for some reason, don't present in the conventional electrolyte solutions at ambient temperature.

Conclusions

For the first time, we obtained the well-defined redox behavior of $Co(CN)_6^{3-/4-}$ in single NaCl microcrystals. The formation mechanism of $Co(CN)_6^{3-}$/NaCl solid solution is confirmed by both crystallographic principle and confocal Raman spectra experiment. The electrochemical investigations show that the electrode process is kinetically controlled, which is elucidated the DFT calculations. DFT results show that reactant, $Co(CN)_6^{4-}$, is stabilized and the active energy of the redox couple, $Co(CN)_6^{3-/4-}$, is lowed in the special dielectric environment NaCl microcrystals. This dielectric-dependent electron transfer behavior recalls the crucial role of dielectric environment of the electrochemical system. A proper dielectric environment can present the electron transfer behavior expected in theory but hardly obtained in experiment. Moreover, the NaCl solid solution is proved a prospective solvent for the solid-state electrochemistry in ambient temperature, which might have potential application in all-in-solid sensors or power sources.

Acknowledgements

Huang, Zhu and Su have equal contributions. The financial supports by the National Science Foundation of China (No. 21327002, 91323303, and 21321062), NFFTBS (No. J1310024), the Natural Science Foundation of Fujian Province of China (No. 2012J06004), and Program for New Century Excellent Talents in University (NCET-12-0318) are appreciated.

References

1 Bard, A. J.; Faulkner, L. R.; *Electrochemical Methods: Fundamentals and Methods*. 2nd ed.; John Wiley & Sons: New York, 2001.

2 Dong, S.; Che, G.; Xie. Y.; *Chemical Modified Electrode*. Second Edition; Science Press: Beijing, 2003.

3 Kotov, V. Y.; Nazmutdinov, R. R.; Botukhova, G. N.; Tsirlina, G. A.; Petrii, O. A.; Hard-to-detect CoIII/CoII reduction in a hexacyanocobaltate. *Mendeleev Commun.* **2004**, *14*, 113-115.

4 (a) Yang, D.; Han, L.; Yang, Y.; Zhao, L. B.; Zong, C.; Huang, Y. F.; Zhan, D.; Tian, Z. Q.; Solid-State Redox Solutions: Microfabrication and Electrochemistry. *Angew. Chem. Int. Ed.* **2011**, *123*, 8838-8841. (b) Zhan, D.; Yang, D.; Yin, B.-S.; Zhang J.; Tian, Z.-Q.; Electrochemical Behaviors of Single Microcrystals of Iron Hexacyanides/NaCl Solid Solution. *Anal. Chem.* **2012**, *84*, 9276-9281. (c) Zhan, D.; Yang, D.; Zhu, Y.; Wu, X.; Tian, Z.-Q.; Fabrication and characterization of nanostructured ZnO thin film microdevices by scanning electrochemical cell microscopy. *Chem. Commun.* **2012**, *48*, 11449-11451.

5 (a) Hassel, A.; Lohrengel, M.; The scanning droplet cell and its application to structured nanometer oxide films on aluminium. *Electrochim. Acta* **1997**, *42*, 3327-3333. (b) Lohrengel, M.; Moehring, A.; Pilaski, M.; Capillary-based droplet cells: limits and new aspects. *Electrochim. Acta* **2001**, *47*, 137-141. (c) Spaine, T. W.; Baur, J. E.; A Positionable Microcell for Electrochemistry and Scanning Electrochemical Microscopy in Subnanoliter Volumes. *Anal. Chem.* **2001**, *73*, 930-938. (d) Rodolfa, K. T.; Bruckbauer, A.; Zhou, D.; Korchev, Y. E.; Klenerman, D.; Two-Component Graded Deposition of Biomolecules with a Double-Barreled Nanopipette. *Angew. Chem. Int. ed.* **2005**, *117*, 7014-7019. (e) Ebejer, N.; Schnippering, M.; Colburn, A. W.; Edwards, M. A.; Unwin, P. R.; Localized High Resolution Electrochemistry and Multifunctional Imaging: Scanning Electrochemical Cell Microscopy. *Anal. Chem.* **2010**, *82*, 9141-9145. (f) Hu, J.; Yu, M.-F.; Meniscus-Confined Three-Dimensional Electrodeposition for Direct Writing of Wire Bonds. *Science*, **2010**, *329*, 313-316.

6 (a) Lai, S.; Patel, A. N.; McKelvey, K.; Unwin, P. R.; Definitive Evidence for Fast Electron Transfer at Pristine Basal Plane Graphite from High-Resolution Electrochemical Imaging. *Angew. Chem. Int. ed.* **2012**, *124*, 5501-5504. (b) Patel, A. N. Collignon, M. G.; O'Connell, M. A.; Hung, W. O.; McKelvey, K., Macpherson, J. V.; Unwin, P. R.; A New View of

Electrochemistry at Highly Oriented Pyrolytic Graphite. *J. Am. Chem. Soc.* **2012**, *134*, 20117-20130. (c) Güell, A. G.; Ebejer, N.; Snowden, M. E.; Macpherson, J. V.; Unwin, P. R.; Structural Correlations in Heterogeneous Electron Transfer at Monolayer and Multilayer Graphene Electrodes. *J. Am. Chem. Soc.* **2012**, *134*, 7258-7261.

7 (a) Patten,H. V.; Lai, S. C.; Macpherson, J. V.; Unwin, P. R.; Active Sites for Outer-Sphere, Inner-Sphere, and Complex Multistage Electrochemical Reactions at Polycrystalline Boron-Doped Diamond Electrodes (pBDD) Revealed with Scanning Electrochemical Cell Microscopy (SECCM). *Anal. Chem.* **2012**, *84*, 5427-5432. (b) Patel, A. N.; McKelvey, K.; Unwin, P. R.; Nanoscale Electrochemical Patterning Reveals the Active Sites for Catechol Oxidation at Graphite Surfaces. *J. Am. Chem. Soc.* **2012**, *134*, 20246-20249.

8 (a) Klemm, S. O.; Kollender, J. P.; Walter Hassel, A. Combinatorial corrosion study of the passivation of aluminium copper alloys. *Corros. Sci.* **2011**, *53*, 1-6;(b) Mardare, A. I.; Ludwig, A.; Savan, A.; Wieck, A. D.; Hassel, A. W. Combinatorial investigation of Hf–Ta thin films and their anodic oxides. *Electrochim. Acta* **2010**, *55*, 7884-7891. (c) Fushimi, K.; Yamamoto, S.; Ozaki, R.; Habazaki, H. Cross-section corrosion-potential profiles of aluminum-alloy brazing sheets observed by the flowing electrolyte scanning-droplet-cell technique. *Electrochim. Acta* **2008**, *53*, 2529-2537.

9 (a) Okunola, A. O.; Nagaiah, T. C.; Chen, X.; Eckhard, K.; Schuhmann, W.; Bron, M. Visualization of local electrocatalytic activity of metalloporphyrins towards oxygen reduction by means of redox competition scanning electrochemical microscopy (RC-SECM). *Electrochim. Acta* **2009**, *54*, 4971-4978. (b) Chen, X.; Eckhard, K.; Zhou, M.; Bron, M.; Schuhmann, W., Electrocatalytic Activity of Spots of Electrodeposited Noble-Metal Catalysts on Carbon Nanotubes Modified Glassy Carbon. *Anal. Chem.* **2009**, *81*, 7597-7603. (c) Lai, S. C.; Dudin, P. V.; Macpherson, J. V.; Unwin, P. R. Visualizing Zeptomole (Electro)Catalysis at Single Nanoparticles within an Ensemble. *J. Am. Chem. Soc.* **2011**, *133*, 10744-10747.

10 (a) Fisher, L.; Israelachvili, J. Direct experimental verification of the Kelvin equation for capillary condensation. *Nature,* **1979**, *277*, 548-549; (b) Fisher, L. R.; Israelachvili, J. N. Experimental studies on the applicability of the Kelvin equation to highly curved concave menisci. *J. Colloid Interface Sci.* **1981**, *80*, 528-541.

11 [11]Carter, D. J.; Ogden, M. I.; Rohl, A. L. Incorporation of Cyano Transition Metal Complexes in KCl Crystals—Experimental and Computational Studies. *Aust. J. Chem.* **2003**, *56*, 675-678.

12 (a) Itaya, K.; Uchida, I.; Neff,V. D. Electrochemistry of polynuclear transition metal cyanides: Prussian blue and its analogues. *Acc. Chem. Res.* **1986**, *19*, 162-168.(b) Sushko, P. V.; Shluger, A. L.; Baetzold, R. C.; Catlow, C. R.; Embedded cluster calculations of metal complex impurity defects: properties of the iron cyanide in NaCl. *J. Phys. Condens. Mat.*, **2000**, *12*, 8257.

13 Gellings, P. J.; Bouwmeester, H. J. M. *The CRC Handbook of Solid State Electrochemistry*. CRC Press: New York, 1997.

14 Tyurin, R. S.; Lyalikov, Y. S.; Zhdanov, S. I.; Thin-Layer Electrochemistry. *Russ. Chem. Rev.* **1972**, *41*, 1086-1100.

15 (a) D. Zhan.; S. Mao.; Q. Zhao.; Z. Chen.; H. Hu.; P. Jing.; M. Zhang.; Z. Zhu.; Y. Shao. Electrochemical Investigation of Dopamine at the Water/1,2-Dichloroethane Interface. *Anal. Chem.* **2004**, *76*, 4128-4136; (b) D. Zhan; X. Li.; W. Zhan.; F.-R. F. Fan.;A. J. Bard. Scanning Electrochemical Microscopy. 58. Application of a Micropipet-Supported ITIES Tip To Detect Ag+ and Study Its Effect on Fibroblast Cells. *Anal. Chem.* **2007**, *79*, 5225-5231; (c) D. Zhan.; F.-R. F. Fan.; A. J. Bard. The Kv channel blocker 4-aminopyridine enhances Ag+ uptake: A scanning electrochemical microscopy study of single living cells. *PNAS*, **2008**, *105*, 12118-12122; (d) Wang, W.; Zhang, J.; Han, L.; Yang, D.; Zhan, D. Generation/collection mode of SECM with combined probe. *Chin. Chem. Lett.* **2012**, *23*, 86–88; (e) Girma, G.; Yu, L.-J.; Huang, L.; Jin, S.; Wu, D.-Y.; Zhan, D. *Anal. Methods*, **2013**, *5*, 4666- 4670; (e) Nestor, U.; Wen, H.; Girma, G.; Mei, Z.; Fei, W.; Yang, Y.; Zhang, C.; Zhan, D. Facilitated Li+ ion transfer across the water/1,2-dichloroethane interface by the solvation effect. *Chem. Commun.* **2014**, *50*, 1015-1017.

16 (a) Lee, C.; Yang, W.; Parr, R. G. Development of the Colle-Salvetti correlation-energy formula into a functional of the electron density. *Phys. Rev. B* **1988**, *37*, 785. (b) Becke, A. D. Density‐functional thermochemistry. III. The role of exact exchange. *J Chem. Phys.* **1993**, *98*, 5648-5652; (c) Frisch, M.; Trucks, G.; Schlegel, H.B.; Scuseria, G.; Robb, M.; Cheeseman, J.; Scalmani, G.; Barone, V.; Mennucci, B.; Petersson, G. Gaussian 09, Revision A. 02, Gaussian. Inc., Wallingford, CT, 2009, 200.

17 (a) Krishnan, R.; Binkley, J.S.; Seeger, R.; Pople,J.A. Self-consistent molecular orbital methods. XX. A basis set for correlated wave functions. *J. Chem. Phys.* **1980**, *72*, 650-654 (b) McLean, A.; Chandler,G. Contracted Gaussian basis sets for molecular calculations. I. Second row atoms, Z=11–18. *J. Chem. Phys.* **1980**, *72*, 5639-5648.

18 (a) Hay, P. J.; Wadt, W. R. Ab initio effective core potentials for molecular calculations. Potentials for the transition metal atoms Sc to Hg. *J. Chem. Phys.* **1985**, *82*, 270-283; (b) Wadt, W. R.; Hay, P. J. Ab initio effective core potentials for molecular calculations: Potentials for main group elements Na to Bi. *J. Chem. Phys.* **1985**, *82* , 284-298.

19 (a) Cances, E.; Mennucci, B.; Tomasi, J. A new integral equation formalism for the polarizable continuum model: Theoretical background and applications to isotropic and anisotropic dielectrics, *J. Chem. Phys.* **1997**, *107*, 3032-3041; (b) Cossi, M.; Barone, V.; Mennucci, B.; Tomasi, J. Ab initio study of ionic solutions by a polarizable continuum dielectric model, *Chem. Phys. Lett.* **1998**, *286*, 253-260.